

Isogeometric spectral approximation for elliptic differential operators

Quanling Deng^{a,b,*}, Vladimir Puzyrev^{a,b}, Victor Calo^{a,b,c}

^a*Curtin Institute for Computation, Curtin University, Kent Street, Bentley, Perth, WA 6102, Australia*

^b*Department of Applied Geology, Curtin University, Kent Street, Bentley, Perth, WA 6102, Australia*

^c*Mineral Resources, Commonwealth Scientific and Industrial Research Organisation (CSIRO), Kensington, Perth, WA 6152, Australia*

Abstract

We study the spectral approximation of a second-order elliptic differential eigenvalue problem that arises from structural vibration problems using isogeometric analysis. In this paper, we generalize recent work in this direction. We present optimally blended quadrature rules for the isogeometric spectral approximation of a diffusion-reaction operator with both Dirichlet and Neumann boundary conditions. The blended rules improve the accuracy and the robustness of the isogeometric approximation. In particular, the optimal blending rules minimize the dispersion error and lead to two extra orders of super-convergence in the eigenvalue error. Various numerical examples (including the Schrödinger operator for quantum mechanics) in one and three spatial dimensions demonstrate the performance of the blended rules.

Keywords: differential operator, spectral approximation, isogeometric analysis, optimally-blended quadratures, Schrödinger operator

1. Introduction

Differential eigenvalue problems arise in a wide range of applications, such as the vibration of elastic bodies in structural mechanics and the multi-group diffusion in nuclear reactors [38]. In general, analytical solutions for these problems are impossible and numerical methods are used. Numerical methods for approximating these differential eigenvalue problems lead to a generalized matrix eigenvalue problem, which is then solved numerically. Different numerical methods result in different matrices and the widely-used methods include finite elements [3, 11, 15, 16, 31–33, 38], isogeometric elements [10, 12, 14, 22, 23, 29, 35, 36], discontinuous Galerkin (DG) [2, 26], hybridizable discontinuous Galerkin (HDG) [27], and a recently de-

*Corresponding author

Email addresses: Quanling.Deng@curtin.edu.au (Quanling Deng), Vladimir.Puzyrev@curtin.edu.au (Vladimir Puzyrev), Victor.Calo@curtin.edu.au (Victor Calo)

9 veloped hybrid high-order (HHO) method [13].

10 Early work [11, 33, 38] used conforming finite elements on simplicial meshes and the method demon-
11 strated convergence rates of order h^{2p} for the eigenvalues and of order h^p in the energy norm for the eigen-
12 functions provided that the eigenfunctions are smooth enough. Sharp and optimal estimates of the numerical
13 eigenfunctions and eigenvalues of finite element analysis are established in [4–6]. In [15, 31, 32], the authors
14 studied the spectral approximation of elliptic operators by mixed and mixed-hybrid methods and optimal er-
15 ror estimates were established. Similar results were obtained more recently in [2, 13, 26, 27] using the
16 DG, HDG, and HHO methods. The spectral approximation by the HDG method leads to a convergence of
17 order h^{2p+1} for the eigenvalues. A non-trivial post-processing, which utilizes a Rayleigh quotient, is also
18 examined in [27] numerically which leads to an improved convergence of order h^{2p+2} for $p \geq 1$. The HHO
19 approximation delivers a convergence of order h^{2p+2} for the eigenvalue errors for all polynomial degrees
20 ($p \geq 0$).

21 Isogeometric analysis is a numerical method introduced in 2005 [18, 28]. The spectral approximation
22 of the elliptic operators arising in structural vibrations were investigated using isogeometric analysis in
23 [19, 30] and the method shows improved spectral approximations over the classical finite elements [18].
24 In [30], a duality principle, which induces a bijective map from spectral analysis to dispersion analysis,
25 was established, which unifies the spectral analysis for structural vibrations (eigenvalue problems) and the
26 dispersion analysis for wave propagations. Further advantages of the method on spectral approximation
27 properties are investigated in [29].

28 The recent work in [14, 36] studies both theoretically and numerically the optimally blended quadrature
29 rules [1] for the isogeometric analysis of the Laplace eigenvalue problem. In [14], the authors establish for
30 $p = 1, 2, \dots, 7$ the super-convergence of order h^{2p+2} for the eigenvalue errors while maintaining optimal
31 convergence of orders h^p and h^{p+1} for the eigenfunction errors in the H^1 -seminorm and in the L^2 -norm,
32 respectively. The work [23] introduces the dispersion-minimized mass for isogeometric analysis and gener-
33 alizes the results to arbitrary polynomial degree p . In [35], the authors study the optimally blended quadra-
34 tures for isogeometric analysis with variable continuity. To reduce the computational costs, [22] describes
35 new quadrature rules to replace the optimal blending rules. For the source problems, optimal (Gaussian)
36 quadrature rules were proposed for isogeometric analysis in [7–9].

37 In this work, we generalize the work in [14, 36] to include the reaction effects in the differential operator
38 as well as to consider different boundary conditions. We study numerically the optimal blending quadratures
39 for the generalized differential operator with both Dirichlet and Neumann boundary conditions. We apply

40 the blending rules to approximate the spectrum of the Schrödinger operator.

41 The outline of the rest of this paper is as follows. We first describe the model problem and the isogeo-
 42 metric discretization in Section 2. We introduce classical and blended quadrature rules in Section 3. A brief
 43 dispersion error estimations is presented in this section. Numerical examples are given in Section 4. Finally,
 44 Section 5 summarizes our findings and describes future research directions.

45 2. Problem statement

We consider the second-order differential eigenvalue problem: Find the eigenpair (λ, u) such that

$$\begin{aligned} -\Delta u + \gamma u &= \lambda u \quad \text{in } \Omega, \\ u &= 0 \quad \text{on } \partial\Omega, \end{aligned} \tag{2.1}$$

where $\Delta = \nabla^2$ is the Laplacian, $\gamma = \gamma(x) \in L^2(\Omega)$ is a smooth and non-negative function, and $\Omega \subset \mathbb{R}^d$, $d = 1, 2, 3$ is a bounded open domain with Lipschitz boundary. This problem is a Sturm-Liouville eigenvalue problem (see, for example, [24, 38]) which has a countable infinite set of eigenvalues $\lambda_j \in \mathbb{R}$

$$0 < \lambda_1 < \lambda_2 \leq \dots \leq \lambda_j \leq \dots \tag{2.2}$$

with an associated set of orthonormal eigenfunctions u_j

$$(u_j, u_k) = \int_{\Omega} u_j(x) u_k(x) \, d\mathbf{x} = \delta_{jk}, \tag{2.3}$$

where δ_{jk} is the Kronecker delta which is equal to 1 when $j = k$ and 0 otherwise. The set of all the eigenvalues is the spectrum of the operator. We normalize the eigenfunctions in the L^2 space and hence the eigenfunctions are orthonormal with each other under the scalar inner product. Now, let us define two bilinear forms

$$a(w, v) = \int_{\Omega} \nabla w \cdot \nabla v + \gamma w v \, d\mathbf{x} \quad \text{and} \quad b(w, v) = (w, v) = \int_{\Omega} w v \, d\mathbf{x}, \quad \forall w, v \in H_0^1(\Omega), \tag{2.4}$$

where $H_0^1(\Omega)$ is the Sobolev space with functions vanishing at the boundary $\partial\Omega$. These two inner products are associated with the following energy and L^2 norms

$$\|w\|_E = \sqrt{a(w, w)}, \quad \|w\| = \|w\|_{L^2(\Omega)} = \sqrt{b(w, w)}. \tag{2.5}$$

Using this notation, the eigenfunctions are also orthogonal with each other under the energy inner product, that is,

$$a(u_j, u_k) = (-\Delta u_j + \gamma u_j, u_k) = (\lambda_j u_j, u_k) = \lambda_j (u_j, u_k) = \lambda_j \delta_{jk}, \tag{2.6}$$

46 where we have used the integration by parts on (2.1) and selected the weighting functions to be eigenfunc-
 47 tions.

At the continuous level, the weak formulation for the eigenvalue problem (2.1) is: Find all eigenvalues $\lambda \in \mathbb{R}$ and eigenfunctions $u \in V$ such that,

$$a(w, u) = \lambda b(w, u), \quad \forall w \in H_0^1(\Omega), \quad (2.7)$$

while at the discrete level, the isogeometric analysis for the eigenvalue problem (2.1) is: Find all eigenvalues $\lambda_h \in \mathbb{R}$ and eigenfunctions $u_h \in V_h$ such that,

$$a(w_h, u_h) = \lambda_h b(w_h, u_h), \quad \forall w_h \in V_h(\Omega), \quad (2.8)$$

48 where $V_h \subset H_0^1(\Omega)$ is the solution and test space, which is spanned by the B-spline or non-uniform rational
 49 basis spline (NURBS) basis functions.

Following [21, 34], the definition of the B-spline basis functions in one dimension is as follows. Let $X = \{x_0, x_1, \dots, x_m\}$ be a knot vector with knots x_j , that is, a nondecreasing sequence of real numbers called knots. The j -th B-spline basis function of degree p , denoted as $\phi_p^j(x)$, is defined as

$$\phi_0^j(x) = \begin{cases} 1, & \text{if } x_j \leq x < x_{j+1} \\ 0, & \text{otherwise} \end{cases} \quad (2.9)$$

$$\phi_p^j(x) = \frac{x - x_j}{x_{j+p} - x_j} \phi_{p-1}^j(x) + \frac{x_{j+p+1} - x}{x_{j+p+1} - x_{j+1}} \phi_{p-1}^{j+1}(x).$$

In this paper, we use the B-splines on uniform meshes with non-repeating knots, that is, we use B-splines with maximum continuity. We approximate the eigenfunction as a linear combination of the B-spline basis functions. Using linearity and substituting all the B-spline basis functions for w_h in (2.8) leads to the matrix eigenvalue problem

$$\mathbf{K}\mathbf{U} = \lambda^h \mathbf{M}\mathbf{U}, \quad (2.10)$$

50 where $\mathbf{K}_{ab} = a(\phi_a, \phi_b)$, $\mathbf{M}_{ab} = b(\phi_a, \phi_b)$, and \mathbf{U} is the corresponding representation of the eigenvector as
 51 the coefficients of the B-spline basis functions. For simplicity, the matrix \mathbf{K} (although it contains a scaled
 52 mass) is referred as the stiffness matrix while the matrix \mathbf{M} is referred as the mass matrix, and $(\lambda_h, \mathbf{u}_h)$ is
 53 the unknown eigenpair.

54 3. Blending quadratures and dispersion errors

55 In this section, we present the quadratures as well as their optimal blendings. Following earlier work
 56 [14, 36] and its recent generalization [23], we omit the details to briefly give the dispersion errors for the

57 quadrature rules. The blending rules are optimal in the sense of delivering minimal dispersion error.

58 3.1. Quadrature rules

In practice, we evaluate the integrals involved in $a(w_h, u_j^h)$ and $b(w_h, u_j^h)$ numerically, that is, approximated by quadrature rules. On a reference element \hat{K} , a quadrature rule is of the form

$$\int_{\hat{K}} \hat{f}(\hat{\mathbf{x}}) \, d\hat{\mathbf{x}} = \sum_{l=1}^n \hat{\omega}_l \hat{f}(\hat{n}_l) + \hat{E}_n, \quad (3.11)$$

where $\hat{\omega}_l$ are the weights, \hat{n}_l are the nodes, n is the number of quadrature points, and \hat{E}_n is the error of the quadrature rule. For each element K , we assume that there is an invertible map σ such that $K = \sigma(\hat{K})$, which determines the correspondence between the functions on K and \hat{K} . Assuming J_K is the Jacobian of the mapping, (3.11) induces a quadrature rule over the element K given by

$$\int_K f(\mathbf{x}) \, d\mathbf{x} = \sum_{l=1}^n \varpi_{l,K} f(n_{l,K}) + E_n, \quad (3.12)$$

59 where $\varpi_{l,K} = \det(J_K) \hat{\omega}_l$ and $n_{l,K} = \sigma(\hat{n}_l)$.

60 The quadrature rule is exact for a given function $f(x)$ when the remainder E_n is exactly zero. For
 61 simplicity, we denote by G_m the m -point Gauss-Legendre quadrature rule, by L_m the m -point Gauss-
 62 Lobatto quadrature rule, and by O_p the optimal blending scheme for the p -th order isogeometric analysis
 63 with maximum continuity. In one dimension, G_m and L_m fully integrate polynomials of order $2m - 1$ and
 64 $2m - 3$, respectively (see, for example, [8, 37]).

Applying the quadrature rules to (2.8), we have the approximated form

$$a_h(w_h, \tilde{u}_h) = \tilde{\lambda}_h b_h(w_h, \tilde{u}_h), \quad \forall w_h \in V_h, \quad (3.13)$$

where for $w, v \in V_h$

$$a_h(w, v) = \sum_{K \in \mathcal{T}_h} \left(\sum_{l=1}^{n_1} \varpi_{l,K}^{(1)} \nabla w(n_{l,K}^{(1)}) \cdot \nabla v(n_{l,K}^{(1)}) + \sum_{l=1}^{n_2} \varpi_{l,K}^{(2)} \gamma(n_{l,K}^{(2)}) w(n_{l,K}^{(2)}) v(n_{l,K}^{(2)}) \right) \quad (3.14)$$

and

$$b_h(w, v) = \sum_{K \in \mathcal{T}_h} \sum_{l=1}^{n_3} \varpi_{l,K}^{(3)} w(n_{l,K}^{(3)}) v(n_{l,K}^{(3)}), \quad (3.15)$$

where $\{\varpi_{l,K}^{(j)}, n_{l,K}^{(j)}\}$ with $j = 1, 2, 3$ specifies three (possibly different) quadrature rules. Here, we assume that we apply the same quadrature rules for the L^2 inner products in (3.14) and (3.15). With these quadrature rules, we can rewrite (with slight abuse of the notation) the matrix eigenvalue problem (2.10) as

$$\mathbf{K}\tilde{\mathbf{U}} = \tilde{\lambda}^h \mathbf{M}\tilde{\mathbf{U}}, \quad (3.16)$$

65 where $\mathbf{K}_{ab} = a_h(\phi_a, \phi_b)$, $\mathbf{M}_{ab} = b_h(\phi_a, \phi_b)$, and $\tilde{\mathbf{U}}$ is the corresponding representation of the eigenvector
 66 as the coefficients of the basis functions.

Remark 3.1. For multidimensional problems on tensor product grids, the stiffness and mass matrices can be expressed as Kronecker products of 1D matrices [25]. For example, in the 2D case, assume that γ is a constant. We define $\gamma = \gamma_{2D} = 2\gamma_{1D}$ and let $\phi_p^i(x)\phi_p^j(y)$ and $\phi_p^k(x)\phi_p^l(y)$ be two 2D basis functions. Using the definition (2.4), we calculate

$$\begin{aligned}
 \mathbf{K}_{ijkl} &= a(\phi_p^i(x)\phi_p^j(y), \phi_p^k(x)\phi_p^l(y)) \\
 &= \int_{\Omega} \nabla(\phi_p^i(x)\phi_p^j(y)) \cdot \nabla(\phi_p^k(x)\phi_p^l(y)) + \gamma_{2D}\phi_p^i(x)\phi_p^j(y)\phi_p^k(x)\phi_p^l(y) \, d\mathbf{x} \\
 &= \int_X \left(\frac{\partial\phi_p^i(x)}{\partial x} \frac{\partial\phi_p^k(x)}{\partial x} + \gamma_{1D}\phi_p^i(x)\phi_p^k(x) \right) d\mathbf{x} \int_Y \phi_p^j(y)\phi_p^l(y) \, d\mathbf{y} \\
 &\quad + \int_X \phi_p^i(x)\phi_p^k(x) \, d\mathbf{x} \int_Y \left(\frac{\partial\phi_p^j(y)}{\partial y} \frac{\partial\phi_p^l(y)}{\partial y} + \gamma_{1D}\phi_p^j(y)\phi_p^l(y) \right) d\mathbf{y} \\
 &= \mathbf{K}_{ik}^{1D} \mathbf{M}_{jl}^{1D} + \mathbf{M}_{ik}^{1D} \mathbf{K}_{jl}^{1D},
 \end{aligned} \tag{3.17}$$

where X and Y specify the intervals of each dimension in Ω . Similarly, we obtain

$$\mathbf{M}_{ijkl} = \mathbf{M}_{ik}^{1D} \mathbf{M}_{jl}^{1D}. \tag{3.18}$$

67 Herein, \mathbf{M}_{ij}^{1D} and \mathbf{K}_{ij}^{1D} are the mass and stiffness matrices of the 1D problem with $\gamma = \gamma_{1D}$ in (2.1). We
 68 refer the reader to [20] for the description of the summation rules.

69 3.2. Blended quadratures

Given two quadrature rules $Q_1 = \{\varpi_{l,K}^{(1)}, n_{l,K}^{(1)}\}_{l=1}^{n_1}$ and $Q_2 = \{\varpi_{l,K}^{(2)}, n_{l,K}^{(2)}\}_{l=1}^{n_2}$, the blended quadrature rule, denoted as Q_τ , is defined as

$$Q_\tau = \tau Q_1 + (1 - \tau) Q_2, \tag{3.19}$$

where τ is referred as the blending parameter. Applying the blended rule Q_τ for the integration of a function f , we have

$$\begin{aligned}
 \int_K f(\mathbf{x}) \, d\mathbf{x} &= \tau \left(\sum_{l=1}^{n_1} \varpi_{l,K}^{(1)} f(n_{l,K}^{(1)}) + E_{n_1}^{Q_1} \right) + (1 - \tau) \left(\sum_{l=1}^{n_2} \varpi_{l,K}^{(2)} f(n_{l,K}^{(2)}) + E_{n_2}^{Q_2} \right) \\
 &= \tau \sum_{l=1}^{n_1} \varpi_{l,K}^{(1)} f(n_{l,K}^{(1)}) + (1 - \tau) \sum_{l=1}^{n_2} \varpi_{l,K}^{(2)} f(n_{l,K}^{(2)}) + \left(\tau E_{n_1}^{Q_1} + (1 - \tau) E_{n_2}^{Q_2} \right).
 \end{aligned} \tag{3.20}$$

Thus, the error for the blending rule is the same as blending of the errors, that is,

$$E^{Q_\tau} = \tau E_{n_1}^{Q_1} + (1 - \tau) E_{n_2}^{Q_2}. \tag{3.21}$$

Assuming that Q_1 and Q_2 integrate polynomials up to order k_1 and k_2 , respectively, (3.21) shows that the blending rule integrates polynomials up to order $\min(k_1, k_2)$. For example, in one dimension, the blending rule

$$Q_\tau = \tau G_m + (1 - \tau)L_m \quad (3.22)$$

70 integrates polynomials up to order $2m - 3$.

71 For the dispersion analysis on the Helmholtz equation ($\gamma = 0$, $\lambda = \omega^2$ in (2.1)), the blended rule shows
72 smaller dispersion errors. In fact, the optimal blending of spectral elements and finite elements, which is
73 realized by optimally blended quadratures, leads to two extra order of super-convergence on the dispersion
74 error; see [1]. This fact motivates the work (see [14, 23, 36]) of finding the optimal blending rules for the
75 isogeometric analysis for differential eigenvalue problems (2.1) with $\gamma = 0$. In the following section, we
76 present the dispersion error-minimized blending rules.

77 3.3. Dispersion errors and optimal blending quadratures

Following earlier work [14, 23], based on the dual principle in [30], the dispersion errors of the isogeometric elements using quadratures can be characterized by the eigenvalue errors. For simplicity, we assume that $\gamma = 0$. For C^1 quadratic isogeometric elements (for linear elements, it is the same with the finite element case and we refer the readers to [36]), the relative errors are

$$\begin{aligned} \frac{\lambda_h^{G_3} - \lambda}{\lambda} &= \frac{1}{720}\Lambda^4 + \mathcal{O}(\Lambda^6), \\ \frac{\lambda_h^{L_3} - \lambda}{\lambda} &= -\frac{1}{1440}\Lambda^4 + \mathcal{O}(\Lambda^6), \end{aligned} \quad (3.23)$$

where $\Lambda = \omega h$ with $\omega^2 = \lambda$ and λ_h^Q denotes the approximate eigenvalue while using the quadrature rule Q . The blending of these two rules, that is, $Q_\tau = \tau G_3 + (1 - \tau)L_3$, leads to the error representation

$$\frac{\lambda_h^{Q_\tau} - \lambda}{\lambda} = \frac{2 - 3\tau}{1440}\Lambda^4 + \mathcal{O}(\Lambda^6). \quad (3.24)$$

For $\tau = 2/3$, we obtain the two extra orders in the error representation and we call this case the optimal blending. The error representation of the optimal blending is

$$\frac{\lambda_h^{O_p} - \lambda}{\lambda} = \frac{11}{60480}\Lambda^6 + \mathcal{O}(\Lambda^8). \quad (3.25)$$

78 For C^2 cubic elements, the optimal blending parameter is $\tau = -3/2$ and we refer to [14] for $p \leq 7$
79 and [23] for the general case. The convergence rate for eigenpairs computed using isogeometric elements

80 is $O(\Lambda^{2p})$ as shown in [19]. The optimal blending leads to a $O(\Lambda^{2p+2})$ convergence rate for the relative
 81 eigenvalue errors.

For a constant γ , we redefine the eigenvalue problem (2.1) as

$$\begin{aligned} -\Delta u &= \hat{\lambda}u & \text{in } \Omega, \\ u &= 0 & \text{on } \partial\Omega, \end{aligned} \tag{3.26}$$

where $\hat{\lambda} = \lambda - \gamma$. Once the eigenvalue problem (3.26) is solved using isogeometric elements with optimal blending rules, we post-process the approximated eigenvalue of (2.1) as

$$\lambda_h = \hat{\lambda}_h + \gamma. \tag{3.27}$$

82 In Section 4, we present the numerical studies of the equation (2.1) for variable coefficient γ using
 83 isogeometric analysis with the optimal blending rules.

84 **4. Numerical examples**

85 In this section, we present numerical examples of the one and three dimensional problems described in
 86 Section 2 to show how optimal quadratures reduce the approximation errors in isogeometric analysis.

87 *4.1. 1D results*

88 The 1D elliptic eigenvalue problem (2.1) with $\gamma = 0$ and homogeneous Neumann boundary conditions
 89 has the exact eigenpairs $\lambda_j = j^2\pi^2$, $u_j = \sqrt{2}\cos(j\pi x)$, $j = 1, 2, \dots$. The approximate eigenvalues λ_j^h are
 90 sorted in ascending order and are compared to the corresponding exact eigenvalues λ_j .

91 Figure 4.1 compares the approximation errors of C^1 quadratic isogeometric elements using the standard
 92 Gaussian quadrature and the optimal rule for problem (2.1) with homogeneous Neumann boundary condi-
 93 tions. The use of the optimal quadrature leads to more accurate results. The optimal ratio of blending of the
 94 Lobatto and Gauss quadrature rules in this case is 2:1 ($\tau = 2/3$), which in this particular case coincides with
 95 the ratio proposed by Ainsworth and Wajid [1] for finite-spectral elements of the same polynomial order.
 96 This ratio is different for higher order isogeometric elements [14].

97 Figure 4.2 shows the convergence of the errors in the eigenvalue approximation with C^1 quadratic isoge-
 98 ometric elements. The optimal quadrature rule has two extra orders of convergence in the eigenvalue errors
 99 compared to the standard fully-integrated isogeometric elements. Not only the convergence rate, but also
 100 the errors are significantly lower for the optimal rule.

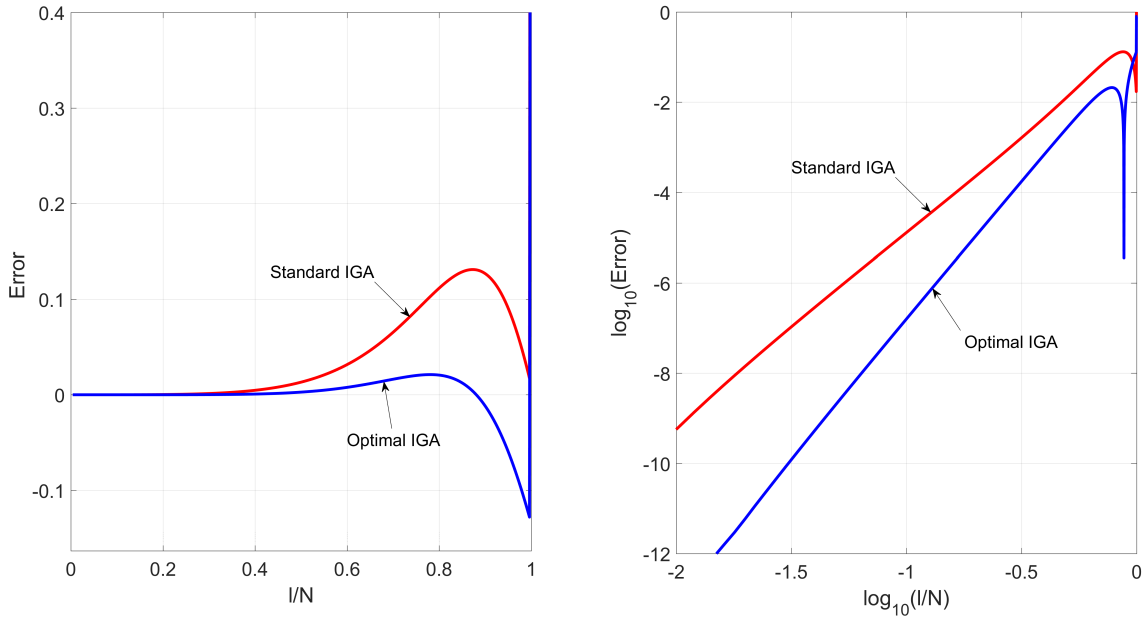


Figure 4.1: Approximation errors for C^1 quadratic isogeometric elements with standard Gauss quadrature rule and optimal rule on linear (left) and logarithmic scales (right). The total number of degrees of freedom (discrete modes) is $N = 1000$.

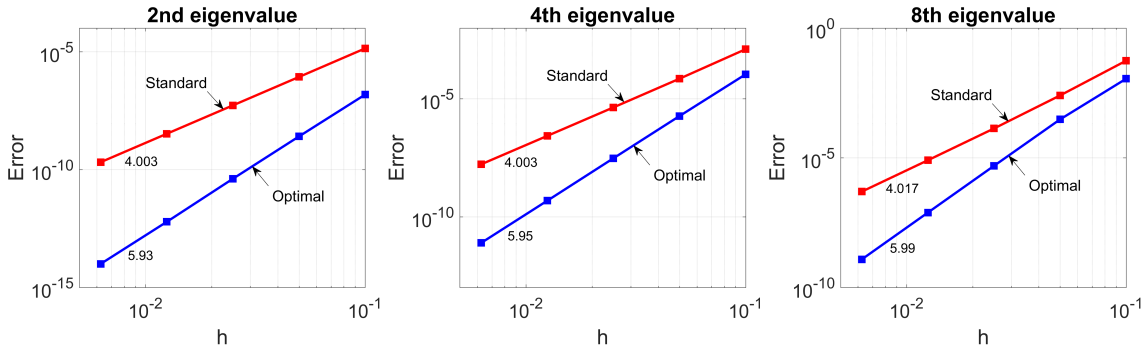


Figure 4.2: Convergence of the errors in the eigenvalue approximation using C^1 quadratic isogeometric elements with standard and optimal quadratures. The second (left), fourth (middle) and eighth (right) eigenvalues are shown.

101 **4.2. 3D results**

Next, we continue our study with the dispersion properties of the three-dimensional eigenvalue problem (2.1) on tensor product meshes. Optimal methods for multidimensional problems with constant coefficients

and affine mappings can be formed by tensor product of the 1D mass and stiffness matrices (3.18). The exact eigenvalues and eigenfunctions of the 3D eigenvalue problem are given by

$$\lambda_{klm} = (k^2 + l^2 + m^2)\pi^2, \quad u_{klm} = 2 \sin(k\pi x) \sin(l\pi y) \sin(m\pi z), \quad (4.28)$$

102 for $k, l, m = 1, 2, \dots$

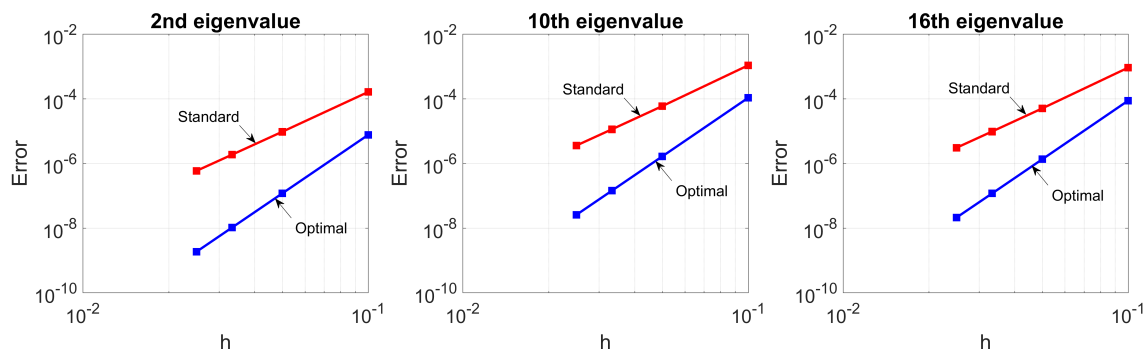


Figure 4.3: Convergence of the errors in the eigenvalue approximation using C^1 quadratic isogeometric elements with standard and optimal quadratures. The second (left), tenth (middle) and sixteenth (right) eigenvalues are shown.

103 Figure 4.3 shows the dispersion errors in the eigenvalue approximation with C^1 quadratic isogeometric
 104 elements. Similar to the 1D case, the optimal scheme has two extra orders of convergence in the eigenvalue
 105 errors.

106 Figure 4.4 compares the eigenvalue errors of the standard Gauss rule using C^1 quadratic elements with
 107 the optimal scheme ($\tau = 2/3$). The latter has significantly better approximation properties in the entire
 108 domain.

109 These results demonstrate that the use of optimal quadratures in isogeometric analysis significantly im-
 110 proves the accuracy of the discrete approximations compared to the fully-integrated Gauss-based method.

111 4.3. Spectral approximation of Schrödinger operator

Following the analytical work on Schrödinger operators in [17], we study their numerical approximations in this subsection. We consider the 1D Schrödinger equation of a quantum particle trapped by the Pöschl-Teller potential

$$\kappa^2 \left(\frac{\alpha(\alpha + 1)}{\cos^2(\kappa y)} + \frac{\beta(\beta + 1)}{\sin^2(\kappa y)} \right), \quad 0 < \kappa y < \frac{\pi}{2}, \quad \alpha, \beta > 0. \quad (4.29)$$

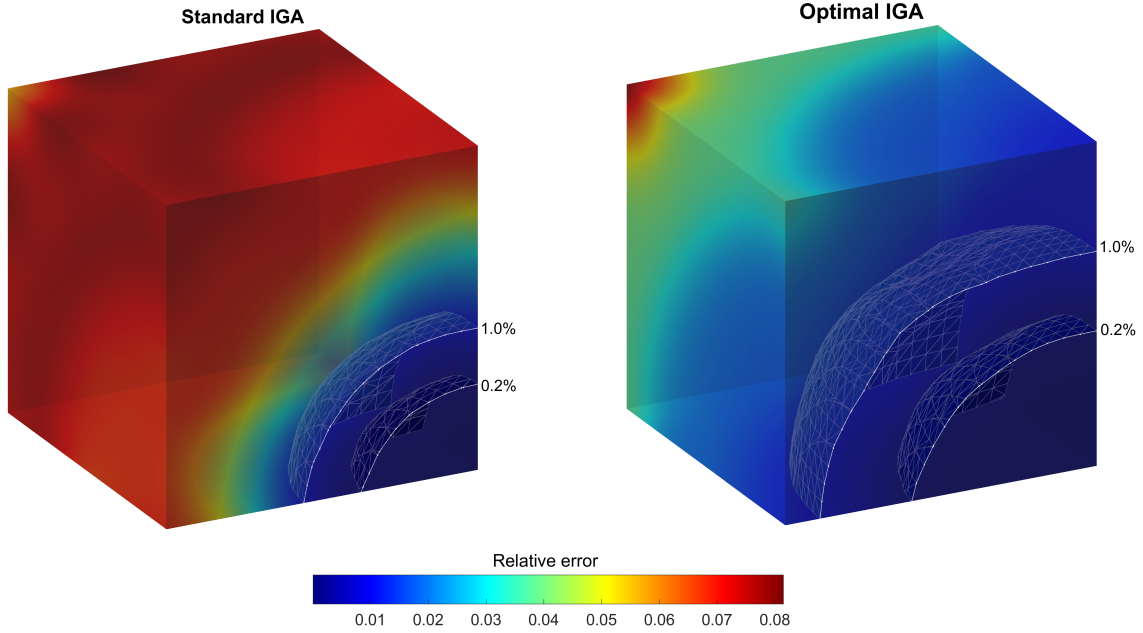


Figure 4.4: Approximation errors for C^1 quadratic isogeometric elements with standard Gauss (left) and optimal quadrature rule (right). Color represents the absolute value of the relative error. Isosurfaces show 0.2% and 1.0% levels of the relative error.

Applying the scaling $x = \kappa y$, the eigenvalue problem reads: Find the eigenpair (λ, u) such that

$$\begin{aligned}
 -\frac{d^2 u}{dx^2} + \left(\frac{\alpha(\alpha+1)}{\cos^2 x} + \frac{\beta(\beta+1)}{\sin^2 x} \right) u &= \lambda u, & 0 < x < \frac{\pi}{2}, \\
 u(0) &= 0, \\
 u\left(\frac{\pi}{2}\right) &= 0,
 \end{aligned} \tag{4.30}$$

where we choose $\alpha = \beta = 1$ for simplicity. This eigenvalue problem has the true eigenvalues (see for example [17])

$$\lambda = (4 + 2j)^2, \quad j = 0, 1, 2, \dots \tag{4.31}$$

112

113 Table 1 shows the relative eigenvalue errors for the first, second and fourth eigenmodes. We present the
 114 errors while using both the Gauss rule and optimally blended rule. Here, since the Pöschl-Teller potential
 115 blows up at the points $x = 0, \frac{\pi}{2}$ and the Lobatto rules utilize the interval element end knots as quadrature
 116 points, we use the G_{p+1} and G_p optimally blended rules (alternatively, one can use the equivalent nonstan-

Set		$ \lambda_1^h - \lambda_1 /\lambda_1$		$ \lambda_2^h - \lambda_2 /\lambda_2$		$ \lambda_4^h - \lambda_4 /\lambda_4$	
p	N	G_{p+1}	O_p	G_{p+1}	O_p	G_{p+1}	O_p
1	40	3.19e-3	6.60e-4	1.06e-2	1.65e-3	3.95e-2	3.81e-3
	80	7.41e-4	8.43e-5	2.49e-3	2.19e-4	9.33e-3	5.97e-4
	160	1.78e-4	1.06e-5	6.04e-4	2.80e-5	2.27e-3	8.07e-5
ρ_1		2.08	2.98	2.07	2.94	2.06	2.78
2	10	1.63e-3	2.65e-4	1.68e-2	4.29e-3	1.02e+0	2.73e-1
	20	7.94e-5	2.39e-6	6.68e-4	6.54e-5	9.07e-3	1.95e-3
	40	4.62e-6	1.11e-7	3.61e-5	5.24e-7	4.07e-4	2.83e-5
ρ_2		4.23	5.61	4.43	6.50	5.64	6.62

Table 1: Relative eigenvalue (EV) errors for C^0 linear and C^1 quadratic isogeometric elements with Gauss rule G_{p+1} and optimally-blended rules O_p .

117 dard quadratures; see [14, 22] for details). The table shows that the eigenvalue errors converge in an order of
118 $2p$ when using the $(p+1)$ -point Gauss rule while the error converges in an order of $2p+1$ and $2p+2$ when
119 using the optimal rule O_p for $p=1$ and $p=2$, respectively. The optimal rules were developed for operators
120 with constant coefficients. It is still an open question to develop optimal rules for the operators with variable
121 coefficients. Herein, for the Schrödinger operator with variable Pöschl-Teller potential, the optimal rules
122 improve the eigenvalue errors significantly but the two-extra orders of convergence are not ensured.

123 5. Conclusions and future outlook

124 We apply the optimally-blended quadrature rules to approximate the spectrum of a general elliptic dif-
125 ferential operator where we account for reaction effects. We show that the optimally blended rules lead to
126 two extra orders of convergence in the eigenvalue errors for both 1D and 3D examples.

127 One future direction is the study on the non-uniform meshes and non-constant coefficient differential
128 eigenvalue problems. The study with variable continuity of the B-spline basis functions is also of interest.
129 We will study the dispersion properties of variable continuity in the basis functions on isogeometric elements
130 and study how the dispersion can be minimized by designing goal-oriented quadrature rules.

131 **Acknowledgement**

132 This publication was made possible in part by the CSIRO Professorial Chair in Computational Geo-
133 science at Curtin University and the Deep Earth Imaging Enterprise Future Science Platforms of the Com-
134 monwealth Scientific Industrial Research Organisation, CSIRO, of Australia. Additional support was pro-
135 vided by the European Union’s Horizon 2020 Research and Innovation Program of the Marie Skłodowska-
136 Curie grant agreement No. 644202, the Mega-grant of the Russian Federation Government (N 14.Y26.31.0013)
137 and the Curtin Institute for Computation. The J. Tinsley Oden Faculty Fellowship Research Program at the
138 Institute for Computational Engineering and Sciences (ICES) of the University of Texas at Austin has par-
139 tially supported the visits of VMC to ICES.

140 **References**

- 141 [1] M. Ainsworth and H. A. Wajid. Optimally blended spectral-finite element scheme for wave propagation
142 and nonstandard reduced integration. *SIAM Journal on Numerical Analysis*, 48(1):346–371, 2010.
- 143 [2] P. F. Antonietti, A. Buffa, and I. Perugia. Discontinuous Galerkin approximation of the Laplace eigen-
144 problem. *Comput. Methods Appl. Mech. Engrg.*, 195(25):3483–3503, 2006.
- 145 [3] I. Babuška and J. Osborn. Eigenvalue problems. In *Handbook of Numerical Analysis, Vol. II*, Handb.
146 Numer. Anal., II, pages 641–787. North-Holland, Amsterdam, 1991.
- 147 [4] U. Banerjee. A note on the effect of numerical quadrature in finite element eigenvalue approximation.
148 *Numerische Mathematik*, 61(1):145–152, 1992.
- 149 [5] U. Banerjee and J. E. Osborn. Estimation of the effect of numerical integration in finite element
150 eigenvalue approximation. *Numerische Mathematik*, 56(8):735–762, 1989.
- 151 [6] U. Banerjee and M. Suri. Analysis of numerical integration in p-version finite element eigenvalue
152 approximation. *Numerical Methods for Partial Differential Equations*, 8(4):381–394, 1992.
- 153 [7] M. Bartoň and V. M. Calo. Gaussian quadrature for splines via homotopy continuation: rules for C2
154 cubic splines. *Journal of Computational and Applied Mathematics*, 296:709–723, 2016.
- 155 [8] M. Bartoň and V. M. Calo. Optimal quadrature rules for odd-degree spline spaces and their appli-
156 cation to tensor-product-based isogeometric analysis. *Computer Methods in Applied Mechanics and*
157 *Engineering*, 305:217–240, 2016.

- 158 [9] M. Bartoň and V. M. Calo. Gauss–Galerkin quadrature rules for quadratic and cubic spline spaces and
159 their application to isogeometric analysis. *Computer-Aided Design*, 82:57–67, 2017.
- 160 [10] M. Bartoň, V. M. Calo, Q. Deng, and V. Puzyrev. *Generalization of the Pythagorean Eigenvalue Error*
161 *Theorem and its Application to Isogeometric Analysis*. To appear, 2017.
- 162 [11] J. H. Bramble and J. E. Osborn. Rate of convergence estimates for nonselfadjoint eigenvalue approxi-
163 mations. *Math. Comp.*, 27(123):525–549, 1973.
- 164 [12] V. Calo, Q. Deng, and V. Puzyrev. Quadrature blending for isogeometric analysis. *Procedia Computer*
165 *Science*, 108:798–807, 2017.
- 166 [13] V. M. Calo, M. Cicuttin, Q. Deng, and A. Ern. Spectral approximation of elliptic operators by the
167 hybrid high–order method. *arXiv preprint arXiv:1711.01135*, 2017.
- 168 [14] V. M. Calo, Q. Deng, and V. Puzyrev. Dispersion optimized quadratures for isogeometric analysis.
169 *arXiv preprint arXiv:1702.04540*, 2017.
- 170 [15] C. Canuto. Eigenvalue approximations by mixed methods. *RAIRO Anal. Numér.*, 12(1):27–50, 1978.
- 171 [16] F. Chatelin. Spectral approximation of linear operators. 1983.
- 172 [17] H. Ciftci, R. L. Hall, and N. Saad. Construction of exact solutions to eigenvalue problems by the
173 asymptotic iteration method. *Journal of Physics A: Mathematical and General*, 38(5):1147, 2005.
- 174 [18] J. A. Cottrell, T. J. R. Hughes, and Y. Bazilevs. *Isogeometric analysis: toward integration of CAD and*
175 *FEA*. John Wiley & Sons, 2009.
- 176 [19] J. A. Cottrell, A. Reali, Y. Bazilevs, and T. J. R. Hughes. Isogeometric analysis of structural vibrations.
177 *Computer methods in applied mechanics and engineering*, 195(41):5257–5296, 2006.
- 178 [20] J. D. De Basabe and M. K. Sen. Grid dispersion and stability criteria of some common finite-element
179 methods for acoustic and elastic wave equations. *Geophysics*, 72(6):T81–T95, 2007.
- 180 [21] C. De Boor. *A practical guide to splines*, volume 27. Springer-Verlag New York, 1978.
- 181 [22] Q. Deng, M. Bartoň, V. Puzyrev, and V. Calo. Dispersion-minimizing quadrature rules for C1 quadratic
182 isogeometric analysis. *Computer Methods in Applied Mechanics and Engineering*, 328:554–564, 2018.

- 183 [23] Q. Deng and V. Calo. Dispersion-minimized mass for isogeometric analysis. *arXiv preprint*
184 *arXiv:1711.02979*, 2017.
- 185 [24] L. C. Evans. *Partial differential equations*, volume 19 of *Graduate Studies in Mathematics*. American
186 Mathematical Society, Providence, RI, second edition, 2010.
- 187 [25] L. Gao and V. M. Calo. Fast isogeometric solvers for explicit dynamics. *Computer Methods in Applied*
188 *Mechanics and Engineering*, 274:19–41, 2014.
- 189 [26] S. Giani. hp-adaptive composite discontinuous Galerkin methods for elliptic eigenvalue problems on
190 complicated domains. *Appl. Math. Comput.*, 267:604–617, 2015.
- 191 [27] J. Gopalakrishnan, F. Li, N.-C. Nguyen, and J. Peraire. Spectral approximations by the HDG method.
192 *Math. Comp.*, 84(293):1037–1059, 2015.
- 193 [28] T. J. R. Hughes, J. A. Cottrell, and Y. Bazilevs. Isogeometric analysis: CAD, finite elements, NURBS,
194 exact geometry and mesh refinement. *Computer methods in applied mechanics and engineering*,
195 194(39):4135–4195, 2005.
- 196 [29] T. J. R. Hughes, J. A. Evans, and A. Reali. Finite element and NURBS approximations of eigenvalue,
197 boundary-value, and initial-value problems. *Computer Methods in Applied Mechanics and Engineer-*
198 *ing*, 272:290–320, 2014.
- 199 [30] T. J. R. Hughes, A. Reali, and G. Sangalli. Duality and unified analysis of discrete approximations
200 in structural dynamics and wave propagation: comparison of p-method finite elements with k-method
201 NURBS. *Computer methods in applied mechanics and engineering*, 197(49):4104–4124, 2008.
- 202 [31] B. Mercier, J. E. Osborn, J. Rappaz, and P.-A. Raviart. Eigenvalue approximation by mixed and hybrid
203 methods. *Math. Comp.*, 36(154):427–453, 1981.
- 204 [32] B. Mercier and J. Rappaz. Eigenvalue approximation via non-conforming and hybrid finite element
205 methods. *Publications des séminaires de mathématiques et informatique de Rennes*, 1978(S4):1–16,
206 1978. Available at http://www.numdam.org/item?id=PSMIR_1978__S4_A10_0.
- 207 [33] J. E. Osborn. Spectral approximation for compact operators. *Math. Comp.*, 29(131):712–725, 1975.
- 208 [34] L. Piegl and W. Tiller. *The NURBS book*. Springer Science & Business Media, 1997.

- 209 [35] V. Puzyrev, Q. Deng, and V. Calo. Spectral approximation properties of isogeometric analysis with
210 variable continuity. *arXiv preprint arXiv:1709.09815*, 2017.
- 211 [36] V. Puzyrev, Q. Deng, and V. M. Calo. Dispersion-optimized quadrature rules for isogeometric anal-
212 ysis: modified inner products, their dispersion properties, and optimally blended schemes. *Computer*
213 *Methods in Applied Mechanics and Engineering*, 320:421–443, 2017.
- 214 [37] J. Stoer and R. Bulirsch. *Introduction to numerical analysis*, volume 12. Springer Science & Business
215 Media, 2013.
- 216 [38] G. Strang and G. J. Fix. *An analysis of the finite element method*, volume 212. Prentice-Hall Englewood
217 Cliffs, NJ, 1973.